

Studying the physics potential of long-baseline experiments in terms of new sensitivity parameters

Mandip Singh*

Department of Physics, Centre of Advanced Study, P. U., Chandigarh, India.

August 25, 2016

Abstract

We investigate physics opportunities to constraint leptonic CP-violation phase δ_{CP} through numerical analysis of working neutrino oscillation probability parameters, in the context of long base line experiments. Numerical analysis of two parameters, the “ transition probability δ_{CP} phase sensitivity parameter (A^M) ” and “ CP-violation probability δ_{CP} phase sensitivity parameter (A^{CP}) ”, as function of beam energy and/or base line has been preferably carried out. It is an elegant technique to broadly analyze different experiments to constraint δ_{CP} phase and also to investigate mass hierarchy in the leptonic sector. The positive and negative values of parameter A^{CP} corresponding to either of hierarchy in the specific beam energy ranges, could be a very promising way to explore mass hierarchy and δ_{CP} phase. The keys to more robust bounds on δ_{CP} phase are improvements of the involved detection techniques to explore bit low energy and relatively long base line regions with better experimental accuracy.

1 Introduction

Phenomenon of neutrino oscillations in vacuum and matter can be described by six fundamental parameters: three lepton flavor mixing angles viz. θ_{12} ; θ_{13} ; θ_{23} , two neutrino mass-squared differences Δm_{21}^2 ; Δm_{23}^2 and one Dirac-type CP-violating phase δ_{CP} , collectively known as neutrino oscillation parameters. Owing to a number of dedicated neutrino oscillation experiments in the past decades, both $(\theta_{12}^2; \Delta m_{21}^2)$ and $(\theta_{23}; |\Delta m_{31}^2|)$ have been measured with reasonably good accuracy [1]. The investigation of moderately large value of smallest leptonic mixing angle θ_{13} in the investigation of lepton mixing matrix [2], [3], [4] by the Daya Bay [5] and RENO [6] reactor neutrino experiments has rejuvenated the opportunities to investigate unknowns in the neutrino physics. This great discovery enhances the possible capability of the next-generation experiments to pin down the neutrino mass hierarchy (i.e., the sign of Δm_{31}^2) and eventually to determine the leptonic Dirac CP-violating phase δ_{CP} . Global fit of neutrino oscillations with data from world class experiments [7], [8] put stringent bounds on the neutrino oscillation parameters.

In the present work we shall discuss about the possible measurement of CP-violating phase ' δ_{CP} ', in the context of recently proposed LAGUNA-LBNO[9] and LBNE[10] experiments.

Long Base Line (LBL) neutrino experiments like LBNO, LBNE etc. due to their long base lines have advantage over the short base line experiments, latter can be approximated to vacuum oscillation neutrino experiments. In vacuum, CP-violation depends only on δ_{CP} phase, hence vacuum oscillation CP-violation amplitudes give pure or intrinsic measurement of δ_{CP} . Due to very small values of CP-violating effects at these short base lines, it is very difficult to carry out their experimental analysis. Over long distances contamination of terrestrial matter effects becomes large, which in turn increases oscillation amplitude and fake the δ_{CP} phase effects. In LBL experiments pure CP-violation effects arising due to δ_{CP} phase only get mixed with CP-violation matter effects arising due to asymmetric forward scattering of neutrino's and anti-neutrino's with matter constituents, also known as fake or extrinsic CP-violation effects. In case of matter oscillation phenomenology, CP conjugate of particle oscillation probability can be obtained by merely changing the sign of δ_{CP} phase and matter potential 'A' (as can be seen in equations (1) and (2) below). Due to these changes, matter effects in the case of normal mass hierarchy produce overall enhancement in the vacuum effects, which makes transition probability amplitude so large at moderate base line lengths that, we expect them to measure experimentally. But now if we shift from the normal mass hierarchy (NH i.e. $\Delta m_{13}^2 > 0$) to the inverted mass hierarchy (IH i.e. $\Delta m_{13}^2 < 0$), the mass hierarchy parameter α in equation (1) also changes sign, due to which a part of matter effects get reduced, which in turn lowers the value of probability amplitude. This addition in the NH-case and subtraction in the IH-case at given base line length 'L' and beam energy 'E', separates the NH and IH probability amplitudes to the amount that we can differentiate among them experimentally.

In LBL experiments, the experimental configurations: LBNE($L = 1280 \text{ km}$, $E = 3.55 \pm 1.38 \text{ GeV}$) and LBNO($L = 2300 \text{ km}$, $E = 5.05 \pm 1.65 \text{ GeV}$) [11] are so chosen, that the asymmetry between $\nu_\mu \rightarrow \nu_e$ and $\bar{\nu}_\mu \rightarrow \bar{\nu}_e$ oscillation probabilities is larger than the CP violation

effects produced by δ_{CP} phase, which makes these suitable for determining the mass hierarchy as well as δ_{CP} phase [12]. The recently proposed neutrino oscillation experiment viz. DUNE [13], [14], [15] with base line nearly equal to LBNE, holds similar discussion and conclusions to that of LBNE. Thus while studying LBNE, we are also studying oscillation phenomenology of the DUNE experiment simultaneously.

2 Oscillation phenomenology of platinum channel

The sub-dominant platinum channel ($\nu_\mu \rightarrow \nu_e$), because of its sensitivity to still unknown neutrino oscillation parameters (e.g. mass ordering, δ_{CP} phase, octant of θ_{23} etc) and ability to analyze experimental data logically, has the advantage over other appearance and disappearance oscillation channels. The analytic expressions for neutrino flavor transition probabilities up to first and/or second order in small oscillation parameters viz. mass ordering parameter (ratio of the solar to atmospheric mass square differences, i.e. $\alpha = \Delta m_{21}^2 / \Delta m_{31}^2$) and third mixing angle ' θ_{13} ' (also known as reactor mixing angle) has been already calculated in the literature by [17], [18], [19] and [20] very elegantly. All these analytic formalisms make use of the method of perturbation theory expansion of neutrino evolution \mathcal{S} -matrix. In the present work, we have preferably made use of the platinum channel oscillation probability from analytic results by [20], that can be written as

$$P_{\mu \rightarrow e} \equiv |S_{e\mu}^f|^2 = \alpha^2 \sin^2 2\theta_{12} c_{23}^2 \frac{\sin^2[A\Delta\frac{L}{2}]}{A^2} + 4 s_{13}^2 s_{23}^2 \frac{\sin^2[(A-1)\Delta\frac{L}{2}]}{(A-1)^2} + 2 \alpha s_{13} \sin 2\theta_{12} \sin 2\theta_{23} \cos(\Delta\frac{L}{2} + \delta_{CP}) \frac{\sin[A\Delta\frac{L}{2}]}{A} \frac{\sin[(A-1)\Delta\frac{L}{2}]}{(A-1)} \quad (1)$$

An another reason for preferring platinum channel lies in the fact, that now a days charged mu-mesons can easily be stored in world class facility accelerator beam dump sources [21], [22], [23], [24], [25], which can be controlled to accelerate these charged entities to the desired energy values.

The transition probability for anti-neutrinos can be obtained by merely changing $\delta_{CP} \rightarrow -\delta_{CP}$ and $V \rightarrow -V$ (or $A \rightarrow -A$) in equation (1) above, hence we can write

$$P_{\bar{\mu} \rightarrow \bar{e}} = \alpha^2 \sin^2 2\theta_{12} c_{23}^2 \frac{\sin^2[A\Delta\frac{L}{2}]}{A^2} + 4 s_{13}^2 s_{23}^2 \frac{\sin^2[(A+1)\Delta\frac{L}{2}]}{(A+1)^2} + 2 \alpha s_{13} \sin 2\theta_{12} \sin 2\theta_{23} \cos(\Delta\frac{L}{2} - \delta_{CP}) \frac{\sin[A\Delta\frac{L}{2}]}{A} \frac{\sin[(A+1)\Delta\frac{L}{2}]}{(A+1)} \quad (2)$$

with $A \equiv 2 E V / \Delta m_{31}^2$, where $V = \sqrt{2} G_F N_e$; with N_e is the number density of electrons in the medium; G_F = Fermi weak coupling constant = $11.6639 \times 10^{-24} \text{ eV}^{-2}$, $\Delta \equiv \Delta m_{31}^2 / 2 E \simeq \Delta m_{32}^2 / 2 E$, $\alpha = \Delta m_{21}^2 / \Delta m_{32}^2$, L is base line length and E the beam energy.

Above Eq. (1) can be rewritten to the form:

$$P_{\mu e} = a + b + c1 \cos \delta_{CP} + c2 \sin \delta_{CP} \quad (3a)$$

with a and b the first and second terms as in Eq. (1) above, these are independent of δ_{CP} phase and the remaining coefficients c1 and c2 of δ_{CP} dependent terms have the following expressions:

$$\begin{aligned} c1 &= 2 \alpha s_{13} \sin 2\theta_{12} \sin 2\theta_{23} \frac{\sin(A\Delta L/2)}{A} \frac{\sin[(A-1)\Delta L/2]}{(A-1)} \cos(\Delta L/2) \\ c2 &= -2 \alpha s_{13} \sin 2\theta_{12} \sin 2\theta_{23} \frac{\sin(A\Delta L/2)}{A} \frac{\sin[(A-1)\Delta L/2]}{(A-1)} \sin(\Delta L/2) \end{aligned} \quad (3b)$$

Eq. (3a) can further be compacted to the following form:

$$P_{\mu e}(\delta_{CP}) = a + b + \sqrt{c1^2 + c2^2} \sin(\beta + \delta_{CP}) \quad (3c)$$

where $\beta = \tan^{-1}(c1/c2)$.

We can analogously compact anti-particle probability given in Eq. (2) to the form similar to the above equation.

Table 1: The best fit and 3σ values of mixing angles and mass square differences from global fit of neutrino oscillation data, adapted from [16].

Parameter	best fit $\pm 1\sigma$	3σ
θ_{12}^o	34.6 ± 1.0	$31.8 - 37.8$
θ_{23}^o [NH]	$48.9^{+1.9}_{-7.4}$	$38.80 - 53.30$
θ_{23}^o [IH]	$49.2^{+1.5}_{-2.5}$	$39.40 - 53.10$
θ_{13}^o [NH]	8.8 ± 0.4	$7.70 - 9.90$
θ_{13}^o [IH]	8.9 ± 0.4	$7.80 - 9.90$
Δm_{21}^2	$7.60^{+0.19}_{-0.18}$	$7.11 - 8.18$
$ \Delta m_{31}^2 _{NH}$	$2.48^{+0.05}_{-0.07}$	$2.30 - 2.65$
$ \Delta m_{31}^2 _{IH}$	$2.38^{+0.05}_{-0.06}$	$2.20 - 2.54$

3 Transition probability, δ_{CP} phase sensitivity parameter (A^M)

This parameter enables us to predict the sensitivity of the transition probability towards the δ_{CP} phase variations for given experimental configuration. We can find the maximum possible transition probability amplitude band width (A^M) for full variation in CP-violation phase δ_{CP} from 0 to 2π radians, at any chosen value of beam energy ‘ E ’ and base line ‘ L ’, with the help of Eq.(3c) to the following form

$$\begin{aligned} \Delta P_{\mu e}^m(\delta_{CP}) &\equiv A^M(\text{say}) \\ &= P_{\mu e}^{max}(\delta_{CP}) - P_{\mu e}^{min}(\delta_{CP}) = 2 \sqrt{c1^2 + c2^2} \end{aligned} \quad (4)$$

A similar type of parameter has been earlier studied in [30, 31, 32]. This parameter is plotted as the green and the yellow colored curves for NH and IH cases respectively in Fig. 1. In the NH-case i.e. green colored curve for LBNE, first oscillation maxima of the parameter A^M lies at 1.6 GeV with value $\approx 5\%$ and second maxima at ≈ 0.8 GeV with value $\approx 10\%$. Similarly for LBNO, first maxima is at 2.8 GeV with value $\approx 6\%$ and second is at ≈ 1.3 GeV with value of $\approx 10\%$. Hence, we can conclude, that both experiments are equally sensitive to the variations in δ_{CP} phase, in the NH-case.

In the IH-case i.e. yellow colored curve for LBNE, the first and second oscillation maximas exist respectively at 2.2 GeV (2%) and 0.9 GeV (7%), where values in parentheses are the corresponding values for the parameter A^M . Similarly for LBNO the first, second and third oscillation maximas are respectively located at 4.2 GeV ($\approx 1\%$), 1.7 GeV ($\approx 6\%$) and 1.0 GeV (11%) respectively.

Thus we can say that in the NH and IH cases, both base lines have almost equal δ_{CP} phase sensitivity at given oscillation maximas. Although for both NH and IH cases, the two base lines have almost equal δ_{CP} phase sensitivity, but location of given oscillation maximas lies at higher values of beam energies in the case of longer base line i.e. LBNO. It is also evident from Fig. 1, that the gradient of parameter A^M w.r.t. the beam energy around peak value of oscillation maxima changes very rapidly (suggesting very fast oscillations) and this rapidness further increases as we move from first to higher order maximas. Owing to this reason, we do not prefer to investigate higher oscillation maximas, yet these have large sensitivity toward δ_{CP} variations. Therefore, we can't investigate higher order maximas with sharp peaks to the desired precision, in the context of currently available energy resolutions of the neutrino detectors.

If we look at the shape of the curves in the shaded region drawn for the spread in beam energy for given experiment, curves are almost straight lines. Due to which, we can predict results in terms of average values over the possible beam energy spreads. We can find from Fig. 1, that $\langle A^M \rangle \approx 2\%$ (NH-case); $\langle A^M \rangle \approx 1\%$ (IH-case) at $\langle E \rangle \approx 3.6$ GeV for LBNE and $\langle A^M \rangle \approx 4\%$ (NH-case); $\langle A^M \rangle \approx 2\%$ (IH-case) at $\langle E \rangle \approx 5.0$ GeV for LBNO. We can conclude, that there is observable sensitivity towards the δ_{CP} phase variations for both experimental configurations, but to achieve more sensitivity towards the variation of δ_{CP} phase and high precision in constraining δ_{CP} phase, we need to explore observable around higher maximas, which can be realized only with nearly mono-energetic beam.

Since in accelerator beam sources both $\bar{\nu}_\mu$ and ν_μ beams are equally available, hence, it is possible to study $\bar{\nu}_\mu \rightarrow \bar{\nu}_e$ channel experimentally. In case of anti-neutrino, Fig. 1 can be replotted by replacing the NH curves with IH ones and vice versa. It is evident from Eq. (1), when we transform from NH-case to IH-case, parameters α , Δ and A change sign, and in the case when we transform from particle to antiparticle, only parameters A and δ_{CP} change sign. If we compare the final results of above two transformations, we can find that it is third term that changes sign, while first two terms appear with same sign in the expressions for two transformations. We can also find that in the chosen beam energy ranges, shown by shaded regions for the two experiments, the contribution of third term is negligible in comparison to sum of first two terms. In Fig. 2, an oscillogram for the parameter A^M in the E - L plane is plotted. It is evident from this figure, that for LBNE in the NH-case, average value (i.e. at

Figure 1: (Color online) The variation in the amplitude of transition probability for platinum channel as a function of beam energy (E). Sub-figure on LHS represents the LBNE ($L = 1,280$ km, $E = 3.55 \pm 1.38$ GeV) and that on RHS to the LAGUNA-LBNO ($L = 2,300$ km, $E = 5.05 \pm 1.65$ GeV) experimental setups, as tabulated in table 2. The green curve corresponds to band width (i.e. parameter A^M) in NH-case and yellow curve in the IH-case, for the full variation (i.e. $0 - 2\pi$) in δ_{CP} phase, as calculated in Eq. (4). The remaining oscillation parameters have the best fit values shown in table 1.

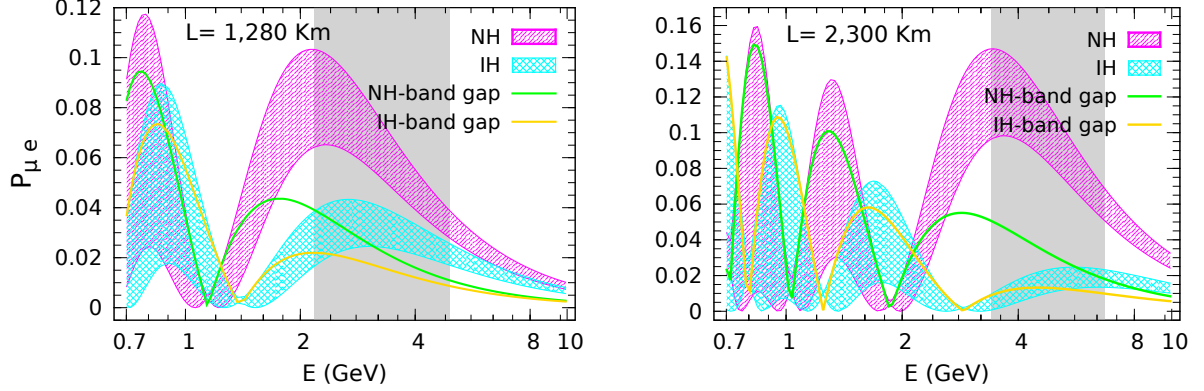
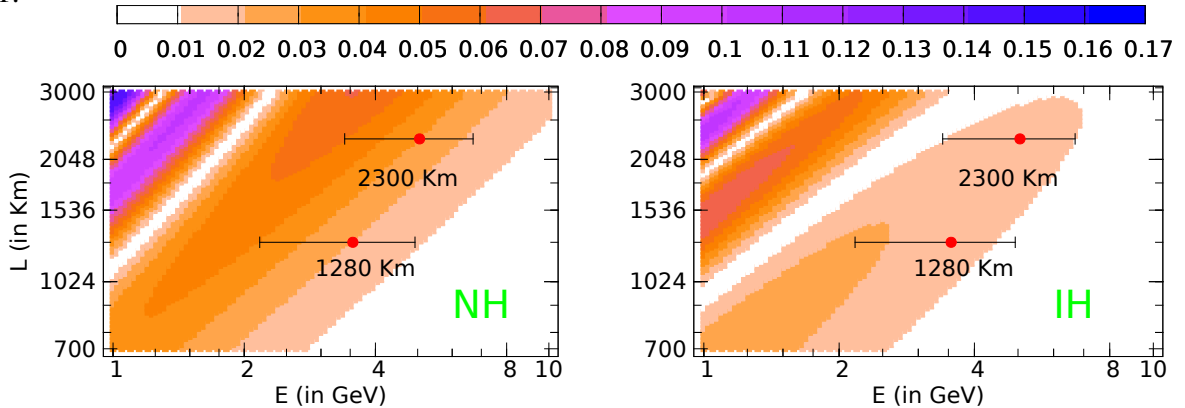


Figure 2: (Color online) An oscillogram of transition probability CP-violation phase sensitivity parameter A^M , in the E - L plane. Central red dot corresponds to $\langle E \rangle$ and error bar to ΔE tabulated in table 2. The remaining oscillation parameters have the best fit values shown in table 1.



central red dot corresponding to average beam energy) of A^M is $\simeq 2\%$, while for IH-case, it is $\simeq 1.5\%$. In the LBNO experiment in the NH-case, the parameter A^M assumes average value of $\simeq 3\%$ while in IH-case, it has value $\simeq 1.5\%$. Hence, in case of both experiments sensitivity toward the variations in δ_{CP} phase for the NH-case is more as compared to the IH-case. Also, this sensitivity further increases at lower end of energy spectrum in case of NH and remains almost same over the whole range in the energy spread for IH-case. It is recommended to investigate the δ_{CP} phase at lower values of energy spectrum, especially for the confirmed NH-case.

Table 2: The Long Base Line (LBL) experimental configurations [11], considered in the present work.

Experiment	Baseline	Beam Energy
	L (km)	$\langle E \rangle \pm \Delta E$ (GeV)
LBNE (DUNE)	1280	3.55 ± 1.38
LBNO	2300	5.05 ± 1.65

4 CP-violation probability, δ_{CP} phase sensitivity parameter (A^{CP})

We can write an expected event rate at detector site in the following way [26, 27, 28, 29]

$$N \simeq \langle \phi P(\nu_\alpha \rightarrow \nu_\beta) \sigma(\nu_\beta \rightarrow \beta) \rangle \quad (5)$$

where angular bracket denotes the average over neutrino beam energy (E_ν), ϕ is the neutrino flux at detector site and σ is the neutrino-nucleon interaction cross section.

Event rate for neutrino and anti-neutrino case from Eq. (5) can be written as

$$N_\nu \simeq \langle \phi_\nu P(\nu_\alpha \rightarrow \nu_\beta) \sigma_\nu \rangle \quad \text{and} \quad N_{\bar{\nu}} \simeq \langle \phi_{\bar{\nu}} P(\bar{\nu}_\alpha \rightarrow \bar{\nu}_\beta) \sigma_{\bar{\nu}} \rangle \quad (6)$$

If we consider the case of nearly mono-energetic neutrino beam, which is true for certain off axis beam and that both the neutrino and anti-neutrino beam fluxes are nearly equal (i.e. $\phi_\nu \simeq \phi_{\bar{\nu}} = \phi$), then we can write

$$\begin{aligned} \Delta N^{CP} &= N_\nu - N_{\bar{\nu}} = \phi \sigma (2 P_{\alpha\beta} - P_{\bar{\alpha}\bar{\beta}}) \\ &\propto 2 P_{\alpha\beta} - P_{\bar{\alpha}\bar{\beta}} = A^{CP}(\text{say}) \end{aligned} \quad (7)$$

where the fact that $\sigma_{\bar{\nu}} \simeq \sigma_\nu/2 = \sigma$, [26, 27, 33, 34] has been used in the above equation.

We can estimate parameter A^{CP} in case of platinum channel ($\nu_\mu \rightarrow \nu_e$) with the help of Eqs. (1) and (2) to the final form as:

$$\begin{aligned}
A^{CP} &= 2 P_{\mu e}(\delta_{CP}) - P_{\bar{\mu} \bar{e}}(\delta_{CP}) \\
&= \alpha^2 \sin^2 2\theta_{12} c_{23}^2 \frac{\sin^2 [A\Delta\frac{L}{2}]}{A^2} + 4 s_{13}^2 s_{23}^2 \left[\frac{2 \sin^2[(A-1)\Delta\frac{L}{2}]}{(A-1)^2} - \frac{\sin^2[(A+1)\Delta\frac{L}{2}]}{(A+1)^2} \right] \\
&\quad + 2 \alpha s_{13} \sin 2\theta_{12} \sin 2\theta_{23} \frac{\sin [A\Delta\frac{L}{2}]}{A} \left[2 \cos(\Delta\frac{L}{2} + \delta_{CP}) \frac{\sin[(A-1)\Delta\frac{L}{2}]}{(A-1)} \right. \\
&\quad \left. - \cos(\Delta\frac{L}{2} - \delta_{CP}) \frac{\sin[(A+1)\Delta\frac{L}{2}]}{(A+1)} \right] \\
&= g + r1 \cos \delta_{CP} + r2 \sin \delta_{CP}
\end{aligned} \tag{8a}$$

where g comprises the first two terms independent of CP-violation phase δ_{CP} and coefficients of the other δ_{CP} dependent terms have the expressions as:

$$\begin{aligned}
r1 &= 2 \alpha s_{13} \sin 2\theta_{12} \sin 2\theta_{23} \frac{\sin [A\Delta\frac{L}{2}]}{A} \left(\frac{2 \sin[(A-1)\Delta L/2]}{A-1} - \frac{\sin[(A+1)\Delta L/2]}{A+1} \right) \cos(\Delta L/2) \\
r2 &= -2 \alpha s_{13} \sin 2\theta_{12} \sin 2\theta_{23} \frac{\sin [A\Delta\frac{L}{2}]}{A} \left(\frac{2 \sin[(A-1)\Delta L/2]}{A-1} + \frac{\sin[(A+1)\Delta L/2]}{A+1} \right) \sin(\Delta L/2)
\end{aligned} \tag{8b}$$

This parameter enables the measurement of CP-violation phase as long as the constant matter density approximation holds very well. Matter effects along with increasing the oscillation amplitude also increase the sensitivity toward the δ_{CP} phase variations. Above Eq. (8a) can be further compacted to the new form, in the following way

$$A^{CP} = g + \sqrt{r1^2 + r2^2} \sin(\gamma + \delta_{CP}) \tag{8c}$$

where $\gamma = \tan^{-1}(r1/r2)$.

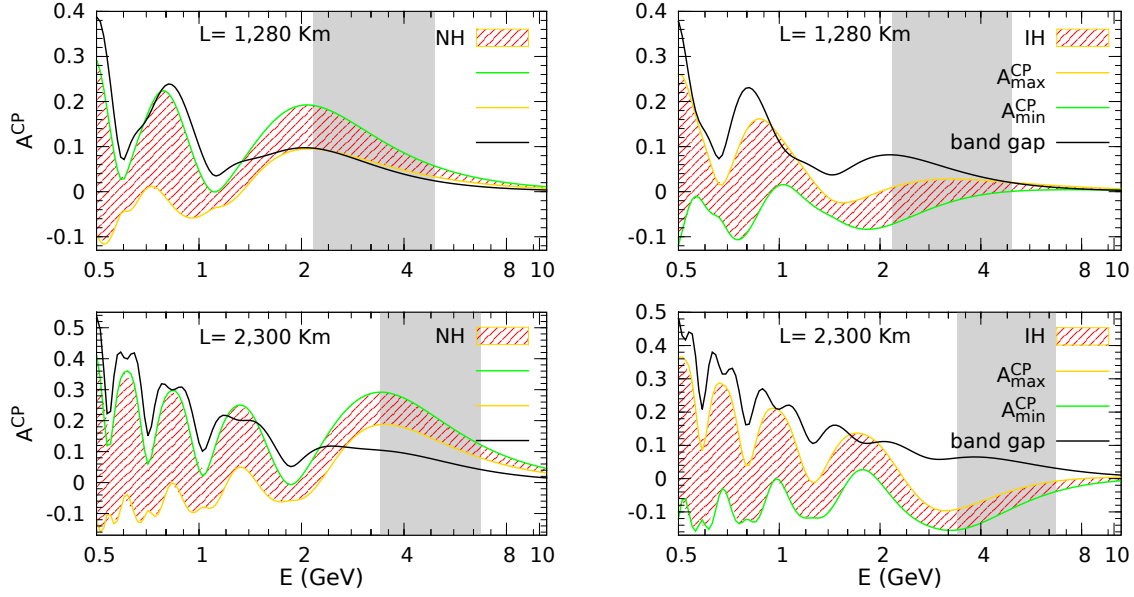
The maximum possible δ_{CP} phase sensitivity of the above CP-violation probability parameter at given beam energy ‘ E ’ and base line ‘ L ’ can be written as:

$$A_m^{CP}(say) \equiv A_{max}^{CP}(\delta_{CP}) - A_{min}^{CP}(\delta_{CP}) = 2 \sqrt{r1^2 + r2^2} \tag{9}$$

this parameter helps to find an optimal beam energy for given base line and the optimal experimental base line for given beam energy, for which δ_{CP} phase sensitivity is maximum. This CP-violation probability, δ_{CP} phase sensitivity parameter A^{CP} (for $\delta_{CP} \rightarrow 0, 2\pi$) in case of both the NH and IH cases, is illustrated as a function of beam energy E in Fig. 3, for the chosen LBL experimental setups viz. LBNE & LBNO.

We will restrict our discussion mainly to and nearby the first oscillation maxima, i.e. for $E > 1$ GeV in case of LBNE and $E > 2$ GeV in the LBNO case. In these figures we

Figure 3: (Color online). Variation of the working parameters; A^{CP} defined in Eq. (8c) [shown by magenta colored band for $0-2\pi$ variation in the δ_{CP} -phase] and maximum possible δ_{CP} phase sensitivity parameter i.e. A_m^{CP} (band width) calculated in Eq. (9) [shown by black curve], as a function of the beam energy E . Thus A_m^{CP} is a measure of band width in the broad curve. The remaining oscillation parameters have the best fit values shown in table 1.



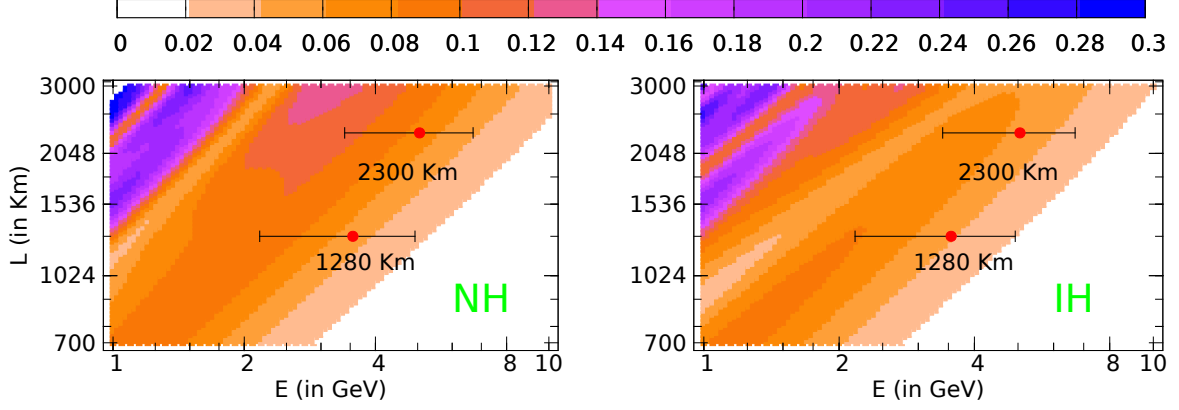
observe that in both the NH and IH cases, for LBNE we expect an average sensitivity of $\approx 3\%$ at $\langle E \rangle \approx 3.55$ GeV and for LBNO there is a sensitivity of $\approx 6\%$ at $\langle E \rangle \approx 5.05$ GeV.

There are other oscillation maximas, for example, at $E \approx 0.8$ GeV with sensitivity of $\approx 25\%$ for LBNE in both the NH and IH cases. While for the LBNO experiment at $E=1.3$ GeV we expect a sensitivity of $\approx 20\%$ for NH-case and sensitivity of $\approx 12\%$ for IH-case. Also, there are other oscillation maximas with sensitivity of $\approx 32, 42\%$ for the NH-case and $\approx 20, 30\%$ for IH-case at $0.8, 0.6$ GeV respectively. But due to fast oscillations around these maximas, almost mono-energetic beam energy could only make the experimental realization possible. Energy spreads in the currently available beam sources are relatively broad, due to which we don't prefer to discuss about these oscillation maximas in detail.

The other thing we notice in these figures is that, in the specific beam energy range, parameter A^{CP} attains positive values for one hierarchy and negative for the other hierarchy. For example, in the case of LBNO experiment, in the beam energy range of $2 - 8$ GeV, parameter A^{CP} assumes positive values in the NH-case, while negative values in the IH-case over the whole δ_{CP} ($0 - 2\pi$) possible range. These positive and negative values of the parameter A^{CP} can be confirmed experimentally. Thus these energy ranges provide the opportunity to investigate mass ordering (MO) along with δ_{CP} phase investigation.

In Fig. 4, an oscillogram for the parameter A_m^{CP} in the $E - L$ plane has been shown. It is evident from the oscillogram that, at central red dot for LBNE(DUNE), A_m^{CP} is $\approx 5\%$ for NH-case and $\approx 4\%$ in IH-case. At lower end of the energy spectrum we expect a sensitivity

Figure 4: (Color online) CP violation probability, δ_{CP} phase sensitivity parameter (A_m^{CP}) oscillogram in the $E - L$ plane. Central red dot corresponds to $\langle E \rangle$ and error bar to ΔE tabulated in table 2. The remaining oscillation parameters have the best fit values shown in table 1.



of $\simeq 9\%$, while at higher end of $\simeq 2\%$ for both hierarchies. In the LBNO experiment, in the NH-case, at central red dot $A_m^{CP} \simeq 8\%$ and further has values of $\simeq 11\%$ & $\simeq 4\%$ respectively at lower & higher ends of energy spectrum. While in the IH-case, parameter A_m^{CP} has value $\simeq 5\%$ at central red dot and has values of $\simeq 7\%$ & $\simeq 3\%$ at lower & higher ends of energy spectrum respectively. Thus for LBNO, normal hierarchy has more sensitivity as compared to inverted hierarchy and the sensitivity further increases at lower end of energy spectrum. It suggests that lower energy spectrum ends are more suitable than higher ones to investigate δ_{CP} phase.

5 Sensitivity of A^M & A^{CP} towards mixing angles and mass square differences variations

In Figs. 5, 6 and 7 sensitivity of working parameters A_m^{CP} and A^M toward the 3σ variations in three mixing angles and two mass square differences is illustrated. It is clear from Fig. 5, that parameter A_m^{CP} is feebly sensitive towards the variations in mixing parameters in the chosen range, for both LBNE and LBNO experiments. From the numerical analysis, it can also be confirmed that parameter A^M has also small sensitivity to the variations in mixing parameters for both the experimental configurations.

In Fig. 6, sensitivity of the parameters A_m^{CP} and A^M towards the variations in mixing parameters for experimental configuration ($E = 0.5 \text{ GeV}$, $L = 1280 \text{ km}$) has been illustrated. We can analyze from the figure, that both parameters have small sensitivity towards mixing angles θ_{12} & θ_{23} variations. Parameter A_m^{CP} has noticeable sensitivity towards the θ_{13} variations, while A^M has small sensitivity. Also, the parameter A_m^{CP} has noticeable sensitivity to the Δm_{12}^2 variations, while parameter A^M has small sensitivity. We can easily notice that A_m^{CP} has large sensitivity towards the Δm_{13}^2 variations, while A^M has moderate sensitivity on that parameter. We can conclude that, if we know θ_{13} very precisely, then parameter A_m^{CP} is left sensitive to the

Figure 5: (Color online) The sensitivity of parameter A_m^{CP} within 3σ variations of mixing angles and mass square differences, for experimental configurations LBNE ($E = 3.55 \text{ GeV}$, $L = 1280 \text{ km}$, $\rho = 3 \text{ g/cm}^3$) [in first two columns] and LBNO ($E = 5.05 \text{ GeV}$, $L = 2300 \text{ km}$, $\rho = 3.3 \text{ g/cm}^3$) [in the third and fourth columns]. The parameter $A_m^{CP} \equiv A_m^{CP}(\mu \rightarrow e)$ along the y-axis is in the units of 10^{-2} . All the other oscillation parameters, except the one considered along x-axis, assume the best fit values, as tabulated in table 1.

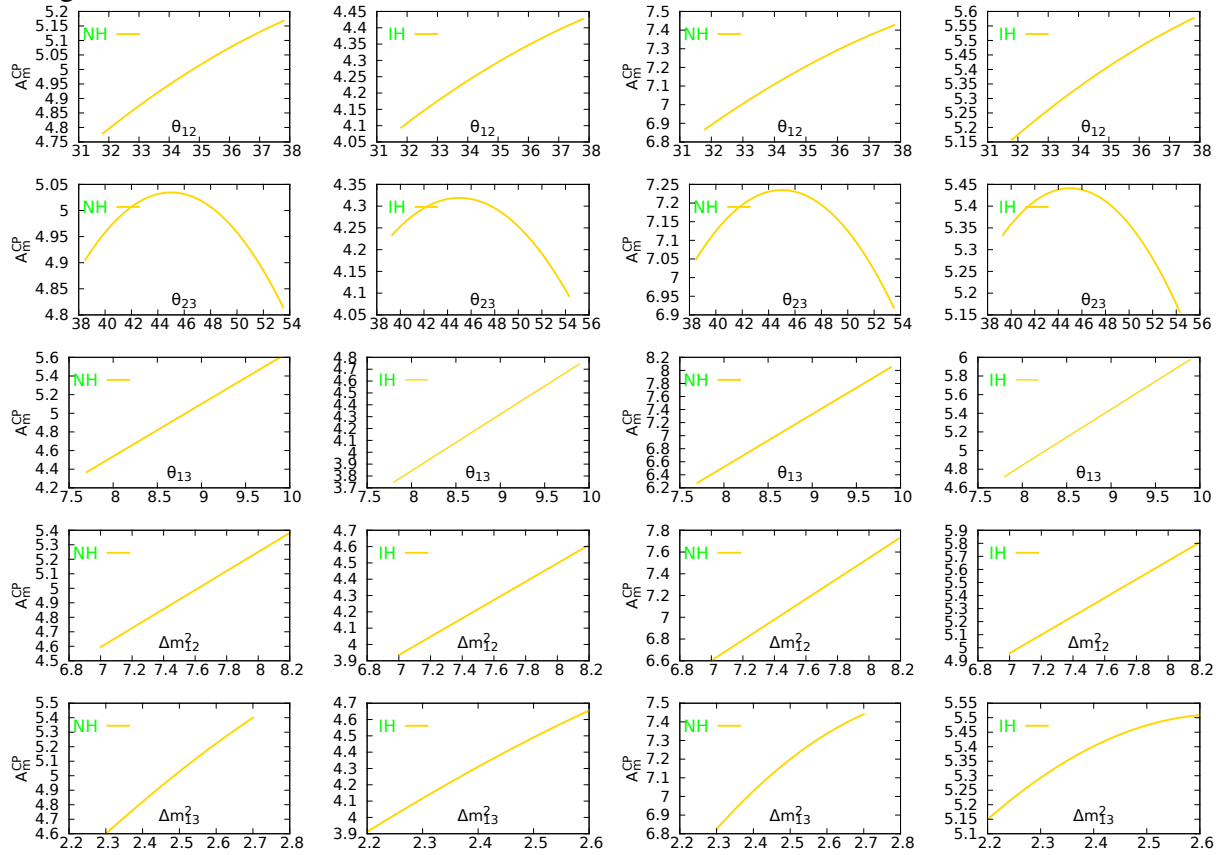


Figure 6: (Color online) The sensitivity of parameters A^{CP} and A^M within 3σ variations of mixing angles and mass square differences, for experimental configuration ($E = 0.5 \text{ GeV}$, $L = 1280 \text{ km}$, $\rho = 3 \text{ g/cm}^3$). The parameter $A_m^{CP} \equiv A_m^{CP}(\mu \rightarrow e)$ along the y-axis is in units of 10^{-2} . Where first column (NH-case) and second column (IH-case) correspond to parameter A^{CP} , while third (NH-case) and fourth (IH-case) columns correspond to the parameter A^M . All other oscillation parameters, except the one considered along x-axis, assume the best fit values, as tabulated in table 1.

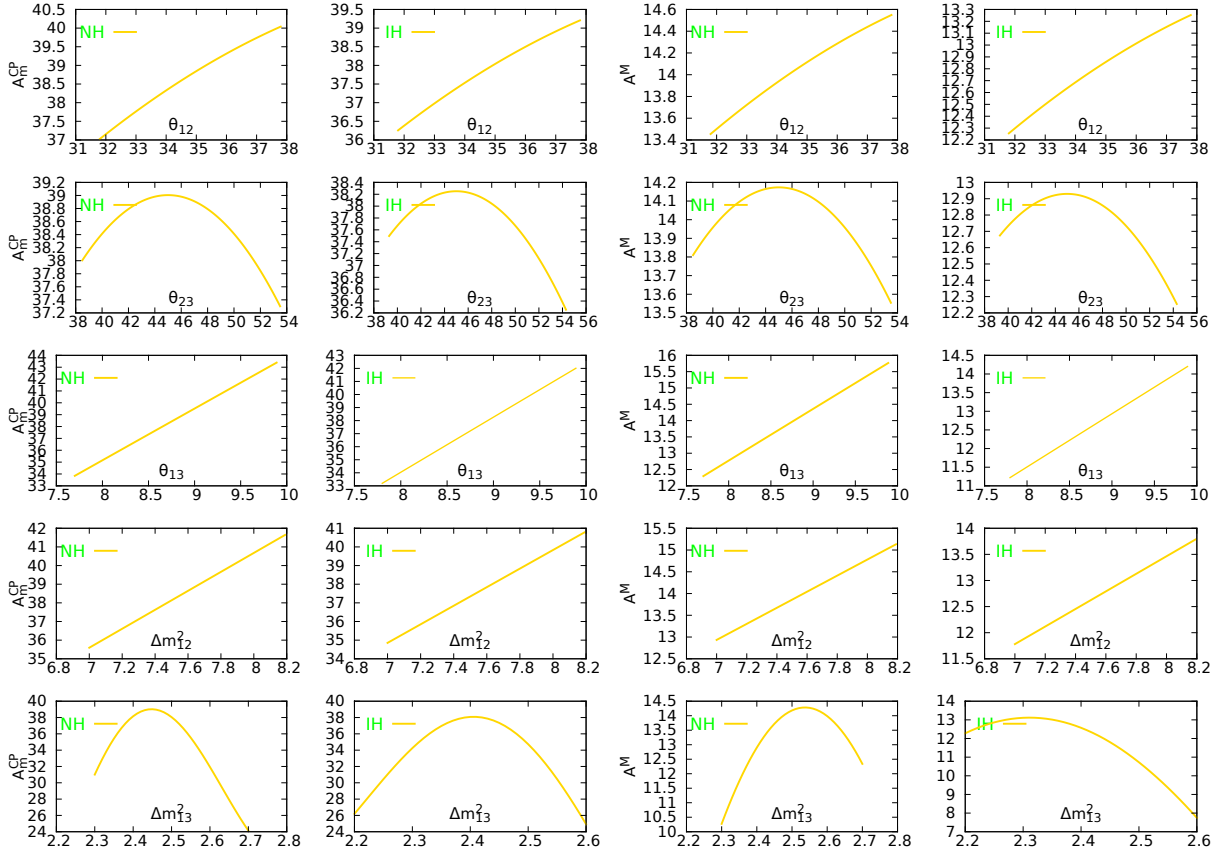
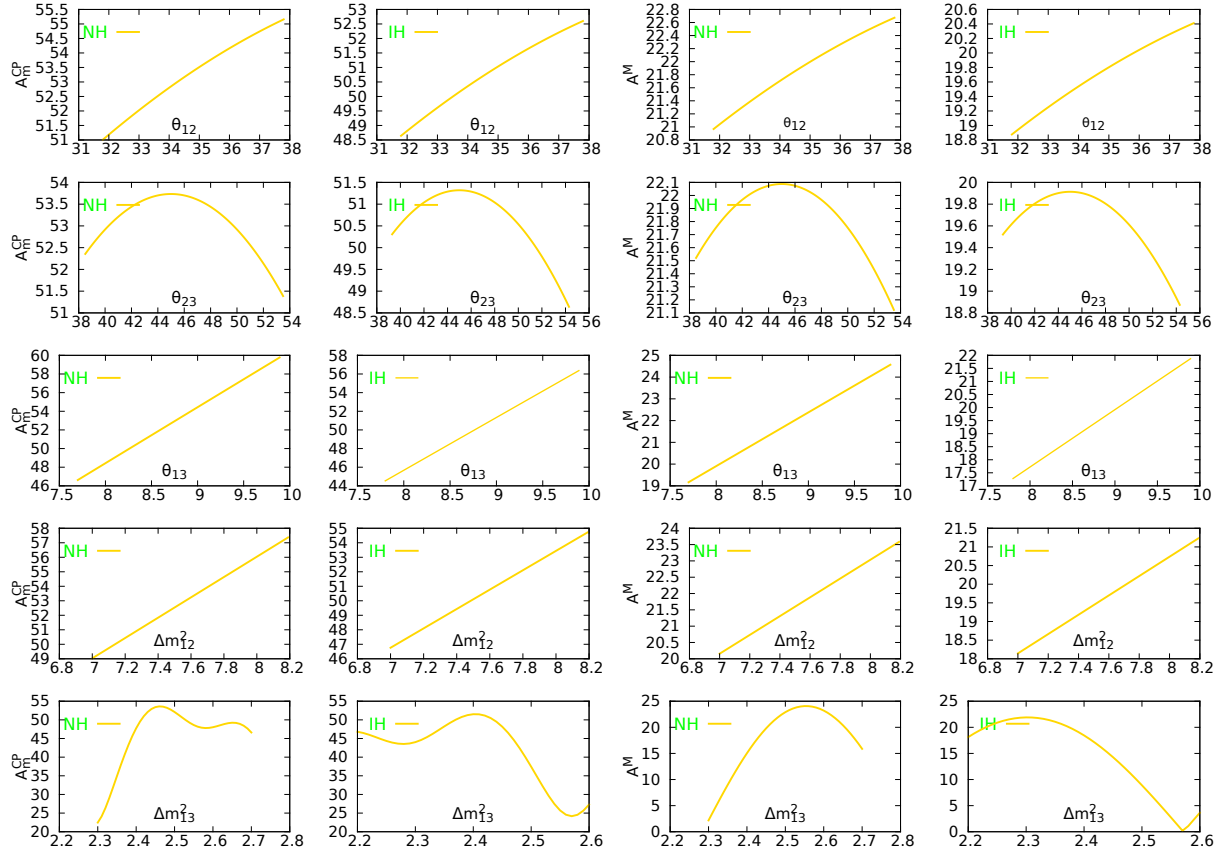


Figure 7: (Color online) The sensitivity of parameter A^M and A_m^{CP} within 3σ variations of mixing angles and mass square differences, for experimental configuration ($E = 0.5 \text{ GeV}$, $L = 2300 \text{ Km}$, $\rho = 3.3 \text{ g/cm}^3$). The parameter $A_m^{CP} \equiv A_m^{CP}(\mu \rightarrow e)$ along the y-axis is in units of 10^{-2} . Where first column (NH-case) and second column (IH-case) correspond to parameter A_m^{CP} , while third (NH-case) and fourth (IH-case) columns correspond to parameter A^M . All the other oscillation parameters, except the one considered along x-axis, assume the best fit values, as tabulated in table 1.



mass square differences.

It is evident from the analysis of Fig. 7 that, parameter A_m^{CP} attains moderate sensitivity towards the θ_{12} and θ_{23} variations, while A^M has small sensitivity towards these variations. Also parameter A_m^{CP} has large sensitivity to the θ_{13} variations, while parameter A^M has moderate sensitivity. Similarly A_m^{CP} has noticeable sensitivity towards the Δm_{12}^2 variations, while A^M has moderate sensitivity. It is evident from figure, that both parameters A_m^{CP} and A^M attain large sensitivity towards the variations in the atmospheric mass square difference (Δm_{13}^2). Thus if we know the precise value of reactor mixing angle θ_{13} then, we are left with large sensitivities of the parameters toward the variations in solar and atmospheric mass square differences only. Parameter A_m^{CP} has large sensitivity towards the solar mass square difference (i.e. Δm_{12}^2) variations in comparison to parameter A^M , while both A_m^{CP} & A^M have large sensitivity towards the variation in atmospheric mass square difference (i.e. Δm_{13}^2) in the 3σ range.

We can also conclude that for given parameter, sensitivity in the NH-case is always almost equal to sensitivity in IH-case. It is also clear from the analysis of all the three Figs. (i.e. 5, 6, 7), that the sensitivity of parameters increase with the increase in baseline length ' L ' and lowering in the beam energy ' E '.

If we compare parameters A_m^{CP} and A^M , then former shows large sensitivity in comparison to latter.

6 Conclusions and perspectives

In this work we have studied two parameters viz. the “ transition probability, δ_{CP} phase sensitivity parameter, A^M ” and the “ CP-violation probability, δ_{CP} phase sensitivity parameter, A^{CP} ” especially to investigate Dirac’s δ_{CP} phase. We can conclude from the analysis of Figs. 1, 2, 3 and 4, that LBNO provides better sensitivity as compared to LBNE towards the δ_{CP} phase variations. We also notice that for a given baseline, this sensitivity is more in the NH-case than in the IH-case, for the parameter A^M . This sensitivity further increases at lower end of energy spectrum. Parameter A^{CP} enables to clearly differentiate among the two mass hierarchies from the positive and negative values of this parameter for either of hierarchy, in the specific beam energy range, as is apparent from Fig. 3. This latter distinction of two hierarchies by the sign of A^{CP} is more pronounced in case of LBNO experiment. We also notice from the comparison of Figs. 2 and 4, that for given base line length (L) and beam energy (E) sensitivity towards the δ_{CP} phase variations is larger for the parameter A_m^{CP} in comparison to parameter A^M .

Though it is not convenient to investigate higher oscillation maximas (i.e., second and third order), due to large spreads in the energy spectrum of beam sources and comparatively less resolutions of the present detectors. But, sufficiently large values of parameters A^M and A_m^{CP} at these maximas encourage to investigate these experimentally, to put more stringent bounds on the δ_{CP} phase. Investigation of these higher oscillation maximas need more accurate detection techniques and almost narrow energy spectra.

At relatively small value of beam energy, ' E ' ($\simeq 0.5$ GeV), sensitivity of the parameter

A_m^{CP} is large towards the atmospheric mass square difference (Δm_{13}^2) variations in case of both LBNE and LBNO experiments. While, this parameter has moderate sensitivity towards the solar mass square difference (Δm_{12}^2) variations, in the LBNE experiment case and has large sensitivity in the case of LBNO. Parameter A^M has moderate sensitivity towards the Δm_{13}^2 variations and has small sensitivity to the Δm_{12}^2 variations in case of LBNE, while this parameter has large sensitivity to Δm_{13}^2 variations and has moderate sensitivity to the Δm_{12}^2 variations in the case of LBNO experiment. Also parameter A_m^{CP} has large sensitivity towards the θ_{13} variations in case of both LBNE and LBNO experiments, while the parameter A^M has moderate sensitivity. In case of both LBNE and LBNO experiments sensitivity of both parameters is small toward the θ_{12} and θ_{23} variations. Thus if we know precise value of reactor mixing angle θ_{13} , we are left with large sensitivities of the parameters toward the variations in solar and atmospheric mass square differences only. If we need large/small sensitivities, we can prefer to low/high beam energy regions.

As parameters A^{CP} & A_m^{CP} are the differences of two CP conjugate channels and parameter A^M is that of single oscillation channel, no doubt errors/uncertainties get canceled to an extent for both parameters, but being a difference involving the same channel such cancellation is large in the case of parameter A^M .

Acknowledgments

I would like to thank Prof. Brajesh Chandra Choudhary (Department of Physics & Astrophysics, Delhi University) for useful discussions.

References

- [1] J. Beringer et al. (Particle Data Group), Phys. Rev. **D 86**, 010001 (2012).
- [2] J. Schechter and J. W. F. Valle, Phys. Rev. **D 22**, 2227 (1980).
- [3] J. Beringer et al. (Particle Data Group), Phys.Rev. **D 86**, 010001 (2012).
- [4] W. Rodejohann and J. Valle, Phys.Rev. **D 84**, 073011 (2011), arXiv:1108.3484 [hep-ph] [Search INSPIRE].
- [5] F. An et al. (Daya Bay Collaboration), Phys. Rev. Lett. **108**, 171803 (2012), arXiv:1203.1669 [hep-ph] [Search INSPIRE].
- [6] J. Ahn et al. (RENO collaboration), Phys. Rev. Lett. **108**, 191802 (2012), arXiv:1204.0626 [hep-ph] [Search INSPIRE].
- [7] M. Gonzalez-Garcia, M. Maltoni, J. Salvado, and T. Schwetz, JHEP **1212**, 123 (2012), arXiv:1209.3023 [hep-ph] [Search INSPIRE].

- [8] F. Capozzi, G. L. Fogli, E. Lisi, A. Marrone, D. Montanino and A. Palazzo, *Phys. Rev. D* **89**, 093018 (2014), arXiv:1312.2878 [hep-ph] [Search INSPIRE].
- [9] S. Bertolucci, A. Blondel, A. Cervera, A. Donini, M. Dracos, D. Duchesneau, F. Dufour and R. Edgecock et al., arXiv:1208.0512 [hep-ex] [Search INSPIRE].
- [10] LBNE Collaboration, Long baseline neutrino experiment collaboration conceptual design report, <http://lbne.fnal.gov/reviews/CD1-CDR.shtml>, (2012).
- [11] T. Ohlsson, H. Zhang, and S. Zhou, arXiv:1301.4333 [hep-ph] [Search INSPIRE].
- [12] D. Dutta, K. Bora, Probing CP violation at LBNE with Reactor experiments, arXiv:1409.8248 [hep-ph] [Search INSPIRE] and references therein.
- [13] R. Acciarri, M. A. Acero, M. Adamowski, C. Adams, P. Adamson S. Adhikari et al., arXiv:1601.05471 [hep-ph] [Search INSPIRE] [physics.ins-det] (2016).
- [14] R. Acciarri, M. A. Acero, M. Adamowski, C. Adams, P. Adamson and S. Adhikari et al., arXiv:1601.02984 [hep-ph] [Search INSPIRE] [physics.ins-det] (2016).
- [15] R. Acciarri, M. A. Acero, M. Adamowski, C. Adams, P. Adamson and S. Adhikari et al., arXiv:1512.06148 [hep-ph] [Search INSPIRE] [physics.ins-det] (2015).
- [16] D. V. Forero, M. Tórtola and J. W. F. Valle, arXiv:1405.7540 [hep-ph] [Search INSPIRE].
- [17] H. Minakata and H. Nunokawa, *JHEP* 0110 (2001) 001, arXiv:hep-ph/0108085 [Search INSPIRE].
- [18] A. Cervera, A. Donini, M. B. Gavela, J. J. Gomez Cadenas, P. Hernandez, O. Mena and S. Rigolin, *Nucl. Phys. B* **579** (2000) 17 [Erratum-ibid. **B 593** (2001) 731] arXiv:hep-ph/0002108 [Search INSPIRE].
- [19] A. M. Gago, H. Minakata, H. Nunokawa, S. Uchinami and R. Zukanovich Funchal, *JHEP* 1001 (2010) **049** [arXiv:0904.3360 [hep-ph] [Search INSPIRE]].
- [20] E. K. Akhmedov, R. Johansson, M. Lindner, T. Ohlsson and T. Schwetz, Series expansions for three-flavor neutrino oscillation probabilities in matter, *JHEP* 0404 (2004) **078** [arXiv:hep-ph/0402175 [Search INSPIRE]].
- [21] W.J. Marciano, Zohreh Parsa, *Nuclear Physics B (Proc. Suppl.)* **221** (2011) 166.
- [22] K. Abe et al. [T2K Collaboration], *Phys. Rev. Lett.* **107**, 041801 (2011).
- [23] R. Patterson (NOvA Collaboration), *Nucl. Phys. Proc. Suppl.* **235**, 151 (2013).
- [24] P. Zucchelli, *Phys. Lett. B* **532**, 166 (2002); M. Mezzetto, *J. Phys. G* **29**, 1771 (2003).
- [25] M. Benedikt, A. Bechtold, F. Borgnolutti, E. Bouquerel, L. Bozyk, et al., *Eur. Phys. J. A* **47**, 24 (2011).

- [26] V. Barger, S. Geer, R. Raja and K. Whisnant, Phys. Rev. D **62**, 013004 (2000).
- [27] V. Barger, S. Geer, and K. Whisnant, arXiv:hep-ph/9906487 [Search INSPIRE].
- [28] M. Freund, M. Lindner, S.T. Petcov and A. Romanino, Nuclear Instruments and Methods in Physics Research A **451** (2000) 18.
- [29] H. Minakata, and H. Nunokawa, arXiv:hep-ph/0009091 [Search INSPIRE].
- [30] K. Kimura, A. Takamura, and T. Yoshikawa, Phys. Lett.B **640**, 32 (2006).
- [31] E. K. Akhmedov, M. Maltoni, and A. Y. Smirnov, JHEP 0705, 077 (2007), arXiv:hep-ph/0612285 [Search INSPIRE].
- [32] E. K. Akhmedov, M. Maltoni, and A. Y. Smirnov, JHEP 0806, 072 (2008), arXiv:0804.1466 [hep-ph] [Search INSPIRE].
- [33] A. Longhina , L. Ludovicib , F. Terranova, arXiv:1412.5987 [hep-ex] [Search INSPIRE].
- [34] M. Freund, P. Huber and M. Lindner, arXiv:hep-ph/0004085 [Search INSPIRE].